European Journal of Mechanics / A Solids 111 (2025) 105533

Contents lists available at ScienceDirect

European Journal of Mechanics / A Solids

journal homepage: www.elsevier.com/locate/ejmsol

Full length article

Tensile strength prediction of fiber-reinforced polymer composites through layered interphase and chemical bonding: A semi-empirical micromechanical model

Jesus A. Rodriguez-Morales [a], Chentong Gao [a,b], Huiyu Sun [a,*]

[a] State Key Laboratory of Mechanics and Control of Mechanical Structures, Nanjing University of Aeronautics and Astronautics, 29 Yudao Street, Nanjing, 210016, China

[b] School of Mechanical and Aerospace Engineering, Nanyang Technological University, 50 Nanyang Avenue, 639798, Singapore

ARTICLE INFO

Keywords:
Mechanical testing
Micromechanics
Interface/interphase
Polymer-matrix composites (PMCs)

ABSTRACT

Fiber-reinforced polymer composites (FRPC) are essential for high-performance applications. However, concerns about their reliability persist owing to their heterogeneous structure across multiple length scales and the critical role of interphases in controlling their performance. In this article, we introduce a semi-empirical micromechanical model that quantitatively considers the impact of chemical treatments on improving interfacial adherence without relying on the Interfacial Shear Strength (IFSS), which is commonly known for posing challenges in characterization. The model predictions across a wide range of FRPC systems are validated against experimental data from the literature, indicating its reasonability and accuracy. Moreover, we analyze the role of parameters affecting fiber–matrix interphase performance, along with a comparison between the Kelly–Tyson model and the modified rule of mixtures. This article provides a simple, practical, and accurate approach to estimating the tensile strength of composite polymer systems and offers insights into the complex role of interphases in overall performance.

1. Introduction

Tensile strength is one of the most critical properties of advanced solid materials for practical applications, as reviewed by Duarte Garcia et al. (2023). For that reason, understanding the maximum allowable load that can be applied to a material without causing significant plastic deformation provides valuable insight into a material's overall strength (Zare, 2014). In the case of polymer composite materials, tensile strength is affected by several factors, including the compatibility between the matrix and the reinforcement, fiber distribution, and interfacial structure and morphology (Kim and Mai, 1998; Jancar, 2008). It is imperative to consider these factors to optimize the tensile strength and durability of the final product. Therefore, an in-depth understanding of the interplay between these elements is necessary to design high-performance polymer composites with superior tensile strength.

Polymer composite materials exhibit viscoelastic behavior, highly susceptible to the interfacial conditions between the polymer and filler (Pan et al., 2013). This implies that interfacial interactions can significantly alter the structure and properties of the polymer present in a thin layer adjacent to the filler surface (Dorigato et al., 2013; Montes-Morán et al., 2005; Montes-Morán and Young, 2002). This thin layer between the polymer and filler, called the interphase, is a crucial aspect of composite materials as it often exhibits mechanical properties distinct from those of bulk materials (see Fig. 1). Several factors influence the interphase, including the interfacial area between the polymer and filler, different surface sizes of the filler, resin curing reaction, and thickness and strength of the interphase (Gu et al., 2010). In particular, the interphase thickness plays a paramount role since an optimized interphase is often associated with stronger interfacial adhesion and, thus, effective stress transfer capabilities (Gu et al., 2010; Gao and Mäder, 2002). For many years, accurately measuring the interphase thickness posed a challenge due to its micro-to-nanometer scale. Nevertheless, powerful optical techniques, including Atomic Force Microscopy (AFM), have proven effective in conducting these measurements even after exposure to detrimental environmental conditions (Gao and Mäder, 2002; Gao et al., 2004; Fard et al., 2020).

Recognizing the importance of optimized interphase, researchers have striven to enhance the interfacial interaction of composites through a series of strategies, using coupling agents that are chemically reactive with both matrix and reinforcement and/or through the

* Corresponding author.
E-mail address: hysun@nuaa.edu.cn (H. Sun).

https://doi.org/10.1016/j.euromechsol.2024.105533
Received 17 July 2024; Received in revised form 4 December 2024; Accepted 5 December 2024
Available online 12 December 2024

chemical modification of the surfaces of one or both constituents (Dey et al., 2014; Ma et al., 2015; Zheng et al., 2022; Liu et al., 2015). Among these strategies, chemical modification is the most frequently employed and effective method for improving interfacial adherence. For example, acid baths and liquid nitrogen oxidation are consistently reported as powerful functionalization methods (Han et al., 2014; Unterweger et al., 2015; Sharma et al., 2014). In these procedures, the surface of the reinforcement is oxidized to enhance the creation of functional groups, often resulting in better adherence to the matrix. However, the majority of these efforts have been limited to experimental work. Two main parameters are typically employed to characterize the fiber–matrix interface: Interfacial Shear Strength (IFSS) and Interfacial Fracture Toughness (IFFT). Methods for characterizing these parameters (e.g., Single Fiber Fragmentation Test (SFFT), pull-out, push-in, and microbond) continue to pose challenges, including labor-intensive specimen preparation, the requirement for specific test setups, and even differences of opinion on the appropriate data reduction schemes (Sørensen and Lilholt, 2016).

On the other hand, analytical efforts to predict the tensile strength of FRPC have primarily relied on shear-lag models (Cox, 1952; Ryu et al., 2003; Mohandesi et al., 2011), laminate analogy approaches (Shokrieh and Moshrefzadeh-Sani, 2017; Yan et al., 2018), Finite Element Analysis (FEA) (Goh et al., 2004; Hashimoto et al., 2012), and, more recently, the bridging model (Huang et al., 2019; Huang and Huang, 2020; Mao et al., 2021). Moreover, an increasing concern about FRPC's reliability under high-temperature applications has prompted multiple studies investigating the effect of interfacial properties on temperature-dependent tensile strength. For example, Sun et al. (2021, 2022) found that the interfacial bonding deteriorates at higher temperatures, leading to a decrease in the reinforcing effect of fibers. The majority of these attempts have been achieved by modifying the rule of mixtures and the maximum shear stress criteria to include partial debonding effects or employing different approaches that combine the bridging model and the Force–Heat Equivalence Energy Density Principle (Li et al., 2018, 2019, 2020; Yang et al., 2021; Zhang et al., 2024). Among these models Li et al. (2020) considered the effect of matrix plasticity, obtaining better agreement with the available experimental data. Additionally, studies based on numerical analysis also demonstrated good comparison with previously reported experimental data (Kundalwal and Kumar, 2016; AhmadvashAghbash et al., 2022; Rivas-Menchi et al., 2024).

Recent studies use micromechanical models to predict tensile strength in unidirectional carbon fiber-reinforced plastics by examining microscale interactions under tensile loading. They focus on stress concentrations around fiber fractures, matrix crack tip opening, and fiber axial stress variations. These approaches capture complex failure behaviors and offer accurate predictions but rely on specific parameters, often limited to brittle PAN-based carbon fibers, highlighting the need for broader applicability (Yamamoto et al., 2019, 2021, 2024). While these models offer a clear physical meaning, incorporating factors such as fiber orientation, length distribution, fiber agglomeration, thermal residual stresses, matrix plasticity, and so on, their mathematical complexity poses challenges, making them cumbersome to solve, computationally expensive, and, more importantly, impractical for engineering applications.

Simpler alternatives, though less efficient, have been commonly employed owing to their practicality. For instance, researchers have widely relied on a rule of mixtures (RoM) or one of their multiple modifications to predict the effective elastic properties of composite systems (Jancar, 2008). A RoM predicts the longitudinal elastic constants relatively well. However, it fails to accurately predict the strength of composite systems owing to its multiple assumptions, overestimating the ultimate tensile strength of unidirectional fiber composites. Consequently, scientists have explored alternative methods for improving prediction accuracy (Rangaraj and Bhaduri, 1994; Lee and Hwang, 1998; Fu and Lauke, 1996; Yang et al., 2019). Among the available

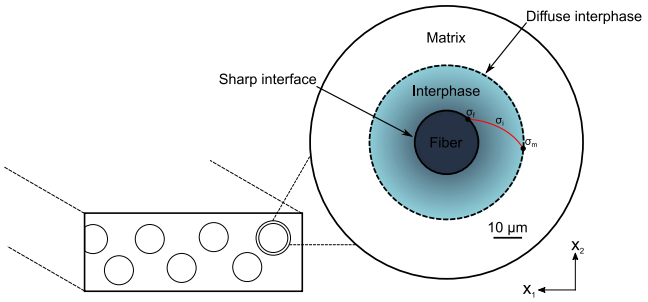

Fig. 1. Schematic representation of Interface/Interphase.

modified RoM (MRoM), the model proposed by Lee and Hwang (1998) led to the most accurate results by introducing a degradation factor. Lee and Hwang concluded that the lack of accuracy of the RoM is due to the difference between the expected and actual contributions of fibers to the composite strength. Alternatively, assuming a plastic matrix and that the IFSS remains constant and equal to the yield strength of the matrix at debond, Kelly and Davies (1965) introduced another widely used model. These assumptions result in the saturation of fiber breaks at a certain load level and a critical fiber length.

Although these theories have been extensively used for predicting the tensile strength of polymer composite systems, overly simplifications, such as the lack of an interphase and perfect interfacial bonding, lead to linear functions and, consequently, poorly accurate predictions at high fiber volume fractions. Nowadays, there is still a significant disparity between the actual strength and analytical calculations of FRPC systems. The key to resolving this issue lies in reasonably optimizing the interphase. In this article, we introduced a semi-empirical micromechanical model that quantitatively considers the effect of chemical bonding on improving interfacial adherence, thereby providing a higher-quality interphase. Our model predictions, spanning a considerable range of composites, have been validated using experimental data from the literature. Additionally, in conjunction with our proposed exponential variable, we analyze the interphase properties that influence the performance of the composites. This model not only provides insights into the complex role of interphases in overall performance but also serves as a valuable tool for designing high-performance composites.

2. Theoretical model

2.1. Basic assumption

The premises of this model include perfectly cylindrical, unidirectional, and uniformly spaced fibers. Further, void elimination and homogeneous fiber volume fraction throughout the composite are needed to ensure a uniform stress distribution. All the phases behave in a linearly elastic way, and the fibers are transversely isotropic. Finally, the interphase has no failure events and a constant thickness.

2.2. Modeling

A micromechanics model is proposed for the strength prediction of fiber-reinforced polymer composites. This model assumes that the composite system is built of small rectangular bodies with square cross-sections, each containing a fiber at its center. Therefore, a single-fiber model is constructed as shown in Fig. 2a. According to the principle of force balance, we have:

$$\sigma_{nc} A = \sigma_{nm} A_m + \sigma_{ni} A_f + \sigma_{ni} A_i \tag{1}$$

where σ_{nc} represents the normal stress on the cross-section of the element; σ_{nm} represents the normal stress on the cross-section excluding

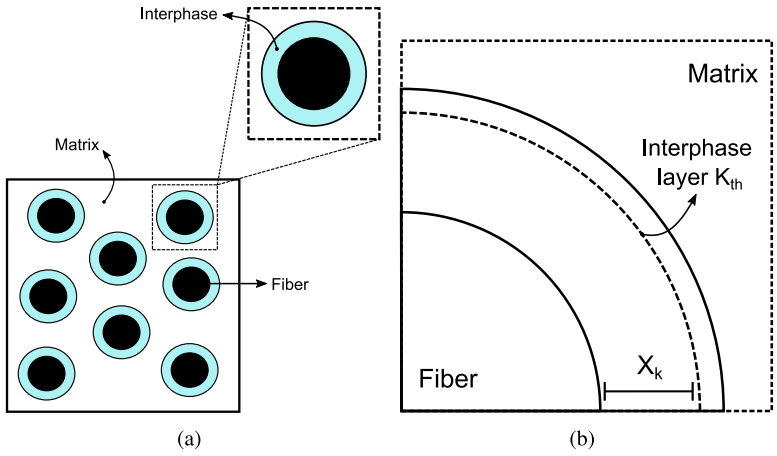

Fig. 2. Schematic illustration of fiber–matrix interphase model (a), and layered interphase strength model (b).

the fiber and interphase; σ_{ni} is the interfacial stress between the fiber and the matrix. A is the cross-sectional area of the element; A_m is the cross-sectional area excluding the fiber's and interphase's area; A_f is the fiber's surface area, and A_i is the cross-sectional area of the interphase. In this case, the interphase stress exhibits a gradient from the matrix to the fiber, primarily influenced by the interfacial adherence. Chemical treatments play a key role in improving this adherence. The closer to the fiber, the more similar the stiffness becomes. In such cases, it is reasonable to assume the surface stress of the fiber and interphase are equal since their deformations would also be equal. This assumption simplifies the analysis by ensuring uniform modeling of stress transfer between the matrix and the fiber. Additionally, as stated by Lee and Hwang, the expected and actual contributions of fibers to the composite strength lead to unrealistic results. Therefore, a proper value adjusted by (σ_{ni}) is intended to display more accurate predictions.

Although it is an approximation, it offers a useful and reasonably accurate representation of the behavior of many practical fiber-reinforced composites. Now, by considering the relationship between geometric parameters and the volume fraction of the fiber, A_f, A_i and A_m are expressed as (see supplementary material for full derivation):

$$A_f = \left(\frac{\pi}{4}\right)^{1/3}\left(\frac{d\phi_f}{l}\right)^{2/3}\cdot A \tag{2}$$

$$A_i = t\pi^{1/3}\left(\frac{4\phi_f}{ld^2}\right)^{2/3}(d+t)\cdot A \tag{3}$$

$$A_m = \left[\left[1-\left(\frac{\pi}{4}\right)^{1/3}\left(\frac{d\phi_f}{l}\right)^{2/3}\right] - t\pi^{1/3}\left(\frac{4\phi_f}{ld^2}\right)^{2/3}(d+t)\right]\cdot A \tag{4}$$

ϕ_f is the fiber volume fraction, l and d are the length and diameter of the fiber, and t is the interphase thickness. For the interphase strength, the model proposed in Zare (2016) is adopted. In his model, the interphase is divided into K layers (see Fig. 2b), each having distinct properties. When the interphase layers have the same thickness, the thickness of the k_{th} layer is expressed as:

$$t_k = \frac{t}{k} \tag{5}$$

X represents the distance from the fiber surface to the polymer matrix. The central point of the k_{th} layer (X_k) is presented as:

$$X_k = k_{th} - \frac{t_k}{2} \tag{6}$$

Therefore, the tensile strength of interphase layers can be changed according to:

$$\sigma_k = \sigma_f - (\sigma_f - \sigma_m)\left(\frac{X_k}{t}\right)^Z \tag{7}$$

σ_f is the tensile strength of the fiber, and Z is an exponent that influences the gradient of the tensile strength across the interphase. In Eq. (7), $\sigma_k = \sigma_f$ at $X_k = 0$ (fiber surface) and $\sigma_k = \sigma_m$ at $X_k = t$ (matrix). At the central layer of the interphase ($X_k = t/2$), we can assume σ_k as the average interphase strength (σ_i). Finally, substituting Eq. (7) into Eq. (1) when ($X_k = t/2$), we obtain:

$$\sigma_c = \sigma_m(1-A_f-A_i) + \left[\sigma_f-(\sigma_f-\sigma_m)\left(\frac{1}{2}\right)^Z\right]A_f + \left[\sigma_f-(\sigma_f-\sigma_m)\left(\frac{1}{2}\right)^Z\right]A_i \tag{8}$$

Eq. (8) integrates the contributions of the matrix, fibers, and interphase to the overall strength of the composite. While Eq. (7) provides reliable interphase strength approximations compared with well-established micromechanics models, as reported by Zare (2016), the appropriate value of the exponent Z is crucial to achieving accurate results. Rather than selecting a scalar value empirically, we propose a simple equation to calculate this exponent.

Although the parameter Z leads to good results when correctly chosen, its random and scattered nature values make it physically ambiguous. Therefore, is necessary a deeper understanding of this parameter and its implications. The exponent Z characterizes how the tensile strength of the interphase layer varies between the fiber and matrix strength across the interphase thickness. Among the parameters affecting Z, we can highlight the effect of chemical treatments, the interplay of mechanical and chemical bonding, interphase thickness, and environmental factors. Given the paramount impact of chemical treatments on the interfacial strength of composite materials, we propose two cases to calculate the new variable Z (see supplementary material for full derivation).

$$Z = \begin{cases} K\cdot\frac{1}{5}\left(\frac{t}{t+1}+n\right), & \text{if } (0 < K \le 1) \\ & \text{(No Chemical Treatment)} \\ \frac{1}{5}+\left(\frac{1}{10}\left(\frac{t}{t+1}+n\right)\right)\cdot(K-1), & \text{if } (1 < K \le 2) \\ & \text{(Chemical Treatment)} \end{cases} \tag{9}$$

Initially, the exponent Z assumes a low value when no chemical treatments are applied in the composite system due to the inherent low compatibility between the constituents. Here, K serves as a variable indicating whether the fibers have undergone chemical treatment, with its value being case-dependent. t represents the interphase thickness, and n functions as a correcting parameter, varying from 0 to 1. The chemical treatment significantly influences the properties of the interphase region in a composite material. Typically, chemical treatments enhance the bonding between fibers and the matrix, modify chemical

compatibility, and affect the mechanical interlocking at the fiber–matrix interface. These improvements manifest in higher values of Z when K exceeds 1. In the following sections, we set the maximum values of K for each case, assuming that untreated composites have moderate interfacial adherence while treated systems show improved stress transfer. A range of K values is proposed for flexibility, given that material compatibility varies. Techniques such as SEM, FTIR, and EDX can qualitatively assess this adherence. In contrast to traditional models that may assume a uniform interphase, this equation allows for a variable transition of properties, providing a more accurate representation of the composite's behavior.

3. Analysis and validation

3.1. Analysis

Parametric analyses can justify the proposed model and demonstrate the dominant factors controlling interphase properties and their influence over composite strength. Eq. (9) describes the correlation between interphase quality, chemical treatments, and interphase thickness. To investigate the impact of these parameters on tensile strength, we analyzed the interplay among these variables.

Fig. 3 exhibits the effect of parameters n and ϕ_f on σ_c using Eq. (8) (σ_m = 40.4 MPa, σ_f = 2600 MPa, t = 300 nm, d = 10 μm, l = 6 mm). For the 3D (Fig. 3a) and contour plots (Fig. 3b); results showed how σ_c increases with n and ϕ_f. However, in the absence of chemical treatments, the increase due to n is less pronounced than the increase due to ϕ_f. This behavior implies that σ_c is more sensitive to changes in ϕ_f than in n as the fiber volume fraction directly contributes to the composite's load-bearing capacity. In the presence of chemical treatments, plots (c) and (d), σ_c shows an important increase. We attribute this increment to interphase's alterations in structure and morphology, promoting enhanced bonding between constituents. Plot (c) suggests that ϕ_f and n contribute to the higher σ_c value, with the effect of ϕ_f even seeming more prevalent. The contour lines in plot (d) are nearly parallel, suggesting that σ_c increases with ϕ_f regardless of the value of n, though the range of σ_c values is much higher in this plot compared to the untreated case.

Fig. 4 shows 3D (Fig. 4a) and contour patterns (Fig. 4b) for the significance of Z and σ_f on the composite strength (σ_m =40.4 MPa, t = 300 nm, d = 10 μm, l = 6 mm t = 40 nm, ϕ_f = 13%) using Eq. (8). The results showed that the lowest values of Z and σ_f led to the worst level of σ_c. However, σ_c improved as these parameters increased, and it reached the highest levels at the greatest levels of Z and σ_f. For instance, a medium Z value of 0.1 and a small σ_f of 2200 MPa result in a composite strength value of 88.55 MPa, similar to the strength of a glass fiber-reinforced composite system. However, as the contour lines become more parallel and narrow with increasing σ_f, the significant influence of the parameter Z becomes evident compared to fiber strength in determining the final composite strength. The growing sensitivity of Z with increasing fiber strength might lead to a denser interphase. This observation supports the idea that strong fibers (high σ_f) do not necessarily introduce strong interphase (high σ_i) at low Z values.

Fig. 5 illustrates the impact of the exponential variable Z on the composite strength σ_c, as indicated by the visible stratification of strength values across the range of Z in the contour plot (Fig. 5b). This suggests that Z is critical in optimizing the composite mechanical performance. While the interphase thickness t contributes to the overall strength, the precise control of Z mainly dictates the composite's capacity to withstand applied loads. Contrary to general consensus, this result supports the idea that thicker interphases do not necessarily improve the load transfer capabilities of composites (Kim et al., 2001; Gao and Mäder, 2002; Downing et al., 2000; Zare, 2016; Papanicolaou et al., 2007). An optimal thickness ensures a sufficient region for load transfer without excessive stress concentrations, while very thin or thicker interphases might compromise their performance, as confirmed in Mäder and Pisanova (2000). Therefore, it is imperative to optimize the interphase thickness to ensure the composite's mechanical properties reflect the fibers' high strength and modulus.

Table 1
Materials information used for short carbon and glass fiber composite systems in Figs. 6 and 7.

Material	Manufacturer	Designation	Length (mm)	Diameter (μm)	Strength (MPa)
SCF	Toho Tenax	HT C604	6	7	4000
SGF	NPG	ChopVantage 3540	6	10	2600

Table 2
Tensile strength (MPa) prediction compared with data reported from Din and Hashemi (1997).

ϕ_f (%)	0	2.2	4.3	9.6	15.3	Error (%)
Experimental	40.4	50.61	52.36	66.36	78.39	–
MRoM	40.4	46.07	52.01	65.17	79.88	2.66
Kelly–Tyson	40.4	46.75	53.40	68.14	84.62	4.05
Our Model	40.4	50.15	56.11	66.43	75.92	2.26

3.2. Validation

Eq. (8) describes the relationship between the tensile strength of fiber-reinforced polymer composites, fiber tensile strength, geometrical parameters, tensile strength of polymer matrices, interfacial strength between constituents, interphase parameters, chemical treatments, and fiber volume fraction.

Din and Hashemi (1997) conducted a study to investigate the influence of short glass fibers on the mechanical properties and fracture behavior of reinforced polycarbonate (PC)/acrylonitrile–butadiene–styrene copolymer (ABS) composites. Tensile strength data from Din and Hashemi's research are utilized in this article for the initial validation of Eq. (8). Given the absence of chemical treatments or any additional coupling agent to enhance interface adhesion, we set K = 1, n = 1/4, and t = 300 nm. In addition, since no details about the mechanical properties of the fiber was provided, we use the technical information in Table 1.

Fig. 6 compares the experimentally measured data, the predictions of our proposed model, the MRoM, and the Kelly–Tyson model for the tensile strength versus the fiber volume fraction. Our model shows a nonlinear increment as the volume fraction increases, and the tensile strength estimations closely match the experimentally measured data. Interestingly, a discrepancy between our predictions and the classical models appears if we continue increasing the volume fraction, as delimited by the vertical dotted line in Fig. 6. We believe this is due to our model's capability of effectively tuning load transfer across the layered interphase. As previously discussed, one of the main factors affecting the tensile strength of FRPC systems is the fiber–matrix interfacial strength. Optimization of elements like surface energy, interfacial chemistry, interphase thickness, and fiber–matrix compatibility is essential to produce stronger interphases (Zheng et al., 2022; Fu et al., 2000). On the other hand, processing conditions, thermal effects, and a high volume fraction make them more susceptible to defects, contributing to a weaker interphase. While classical models do not consider the interplay of these factors within the interphase or simply rely on statistical methods to fit the data, our model accounts for this interrelationship through the parameter K and the exponential variable, leading to more accurate results as we increase the fiber volume fraction.

Moreover, we display the calculated tensile strength values for each model in Table 2. Results further corroborate the outperforms of our model with a minimum error of 2.26% compared with higher values reported by classical models.

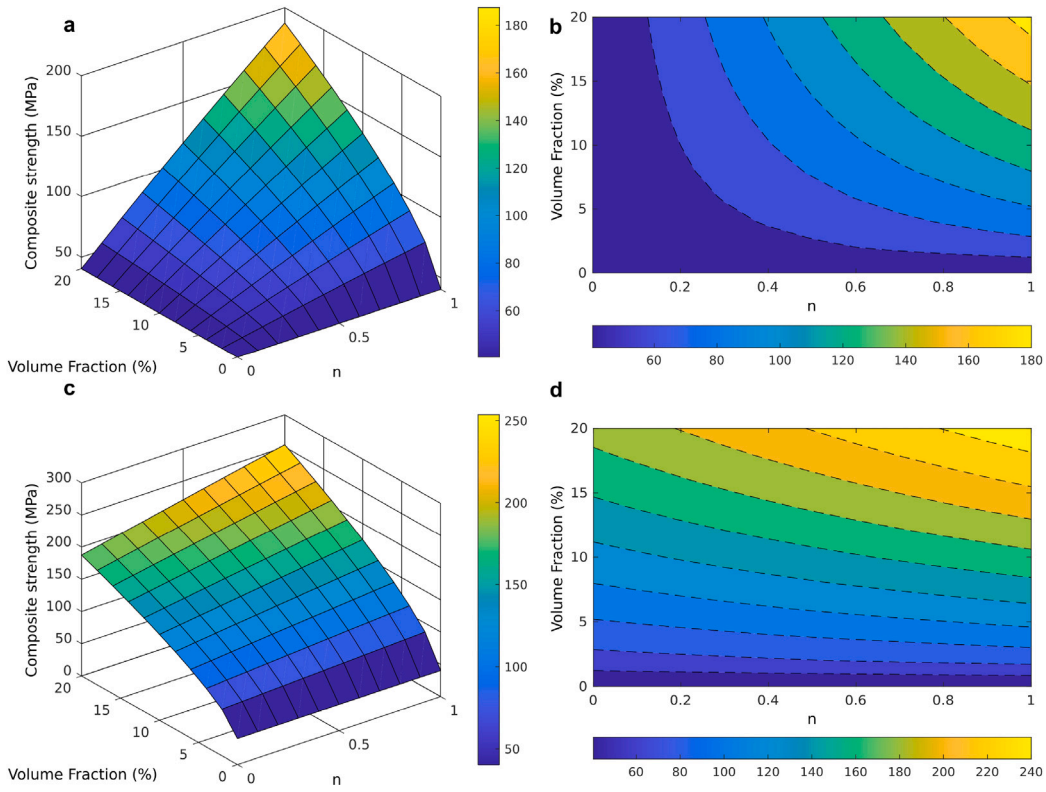

Fig. 3. The effect of parameters "n" and "ϕ_f" on "σ_c" (σ_m = 40.4 MPa, σ_f = 2600 MPa, t = 300 nm, d = 10 μm, l = 6 mm) when there are no chemical treatments: (a) 3D and (b) contour plots, and when there are chemical treatments: (c) 3D and (d) contour plots.

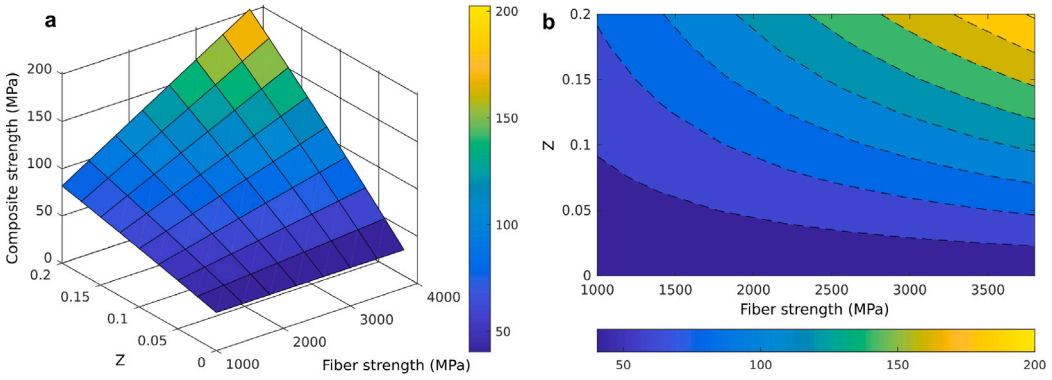

Fig. 4. The effect of parameters "σ_f" and "Z" on "σ_c" (σ_m = 40.4 MPa, t = 300 nm, d = 10 μm, l = 6 mm t = 40 nm, ϕ_f = 13%): (a) 3D and (b) contour plots.

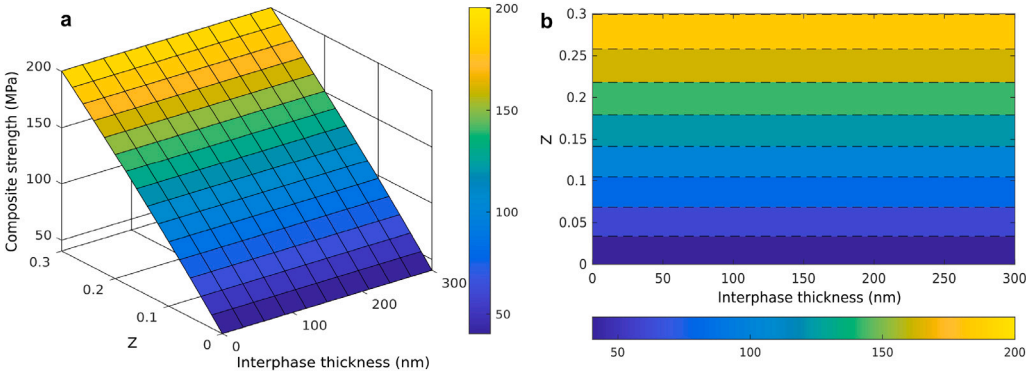

Fig. 5. The effect of parameters "t" and "Z" on "σ_c" using (σ_m = 40.4 MPa, σ_f = 2600 MPa, d = 10 μm, l = 6 mm): (a) 3D and (b) contour plots.

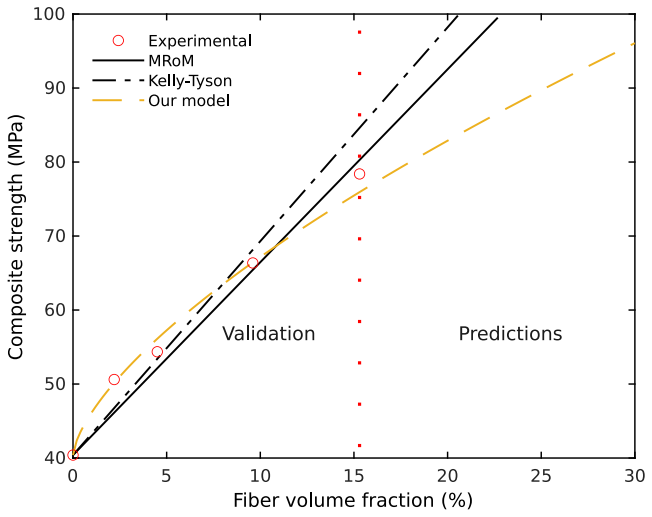

Fig. 6. The calculation of MRoM, Kelly–Tyson and our proposed model compared with experimental data reported in Din and Hashemi (1997) (σ_m = 40.4 MPa, σ_f = 2600 MPa, t = 300 nm (Gao and Mäder, 2002), d = 10 μm, l = 6 mm, K = 1, n = 1/4).

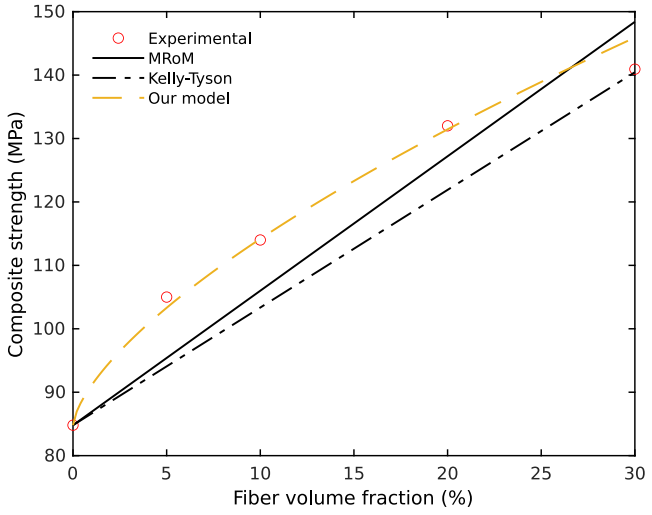

Fig. 7. The calculation of MRoM, Kelly–Tyson, and our proposed model with experimental data reported in Zhao et al. (2018) (σ_m = 84.8 MPa, σ_f = 4000 MPa, t = 40 nm (Gu et al., 2010; Gao et al., 2004), d = 7 μm, l = 6 mm, K = 1, n = 1/4).

Zhao et al. (2018) compared the mechanical and tribological properties of short glass fiber and carbon fiber-reinforced polyethersulfone composites. Here, the tensile strength data from the carbon fiber-reinforced polyethersulfone composite sample is used to validate Eq. (8). The authors found a progressive increment of the tensile strength as they increased the fiber volume fraction, agreeing with the general perception. We maintain the values of K and n as before, but set t = 40 nm, considering that carbon fiber composites typically have a smaller interphase thickness than glass fiber composites (Jancar, 2008; Fu et al., 2000). As in our previous example, we use the data provided in Table 1 for the fiber information.

Fig. 7 compares experimentally measured data and the predicted values from MRoM, Kelly–Tyson, and our proposed model. Despite carbon fibers having chemically inert surfaces and low surface energy, which contribute to poor interfacial performance between constitutes, this drawback becomes evident as we increase the fiber volume fraction (He et al., 2020; Wu et al., 2021). However, our model closely follows the data trend as we increase this parameter. It is generally believed that the mechanical strength of FRPC depends on the fiber–matrix interfacial structure and morphology. Therefore, the capability of our model to capture the nonlinear behavior of these materials allows for better predictions, as the interphase properties now tune the load transfer.

Unterweger et al. (2014) studied experimentally the effect of different fibers on fiber-reinforced polypropylene composites by comparing different sizings and the use of Maleic anhydride-grafted polypropylene (MAPP) as a coupling agent. MAPP has been widely used to improve interfacial adhesion by attaching polar groups produced by maleic anhydride onto the molecular backbone (Yazdani et al., 2006). Unterweger and co-workers found that incorporating MAPP led to an improved composite performance. This enhancement is because adding a coupling agent improves interfacial adhesion, reducing stress concentrations and increasing the energy required to initiate crack formation (Wong et al., 2012). Additionally, a comparison of different fiber sizings demonstrated that the interaction between the fiber and matrix plays a crucial role in composite performance.

Table 3 compares experimentally measured data, predicted values from MRoM, Kelly–Tyson, and our proposed model. In the case of short glass fiber polypropylene (SGF/PP) composite systems, the highest tensile strength value is obtained by adding MAPP and Polyamide (PA) as sizing. As expected, this combination provides the best chemical bonding since PA-sized fibers have a highly polar surface, resulting in better interaction with the coupling agent. Our model captures this phenomenon by adjusting the magnitude of K, thereby influencing Z (refer to supplementary material). Notably, the highest values of Z correspond to the highest tensile strength values, indicating better interfacial properties and positively affecting the strength of the composite material. On the other hand, for short carbon fiber polypropylene (SCF/PP) composites, the best combination resulted in MAPP and Polyurethane (PU) as sizing. This is because PU-sized fibers with higher polar and total surface energy allow better interaction with the coupling agent (Franco-Marquès et al., 2011; Li et al., 2014). Our model showed a consistent correlation as before, obtaining the highest value of Z along with the highest values of tensile strength. Furthermore, the lowest values of Z for both systems are associated with the lowest tensile strength values. This implies a weak interaction between crossover sites of different SCFs in the matrix. As a result, the effective network structure necessary for bearing load was not formed in the PP matrix (Li et al., 2014).

To analyze the universality of our model, we further compared our predictions with different data found in the literature. Fig. 8 shows that our model consistently follows the data trend as the fiber volume fraction increases even after the intersection with the classical models. As Figs. 8d and 6 depict, when this intersection occurs, our model continues increasing in magnitude as we increase the fiber content but more conservatively. This ensures a more realistic estimation when the fiber content is high. However, we delimited a confidence zone where our predictions show their highest accuracy. In any case, our model outperforms the most commonly used models for predicting composite strength.

The data shown in Fig. 8 reflects different composite systems. For example, data from Fig. 8b comes from natural fiber-reinforced composites with an epoxy resin. Owing to the hydrophilic nature of natural fiber and epoxy resin, these fibers were chemically modified with a sodium hydroxide (NaOH) solution to improve interfacial bonding. Data from Fig. 8c, comes from short glass fiber-reinforced composites with a PP matrix. At the same time, data from Fig. 8d comes from glass fiber-reinforced composites with a polyester matrix. In all the cases, plots show consistent data fitting across an acceptable fiber volume content (Data for each system can be consulted on the supplementary material). However, our model limits itself to predicting only the tensile strength of FRPCs. In addition, though we acknowledge that other events influence the behavior of these materials, such as microscopic failure, matrix plasticity, and so on, our model remains simple and accurate for engineering applications.

Table 3
Tensile strength (MPa) prediction compared with data reported from Unterweger et al. (2014) (Interphase thickness values are taken as before).

Sample	ϕ_f(%)	Sizing	d (mm)	l (μm)	Tensile strength	MRoM	Kelly–Tyson	Our model	Z Eq. (9)	σ_f (MPa)	σ_m (MPa)	K	n
SCF[a]/PP	18.1	PA[d]	6	7	45	68.09	71.85	45.89	0.02	4000	28	1	1/10
SCF/PP + MAPP[c]	18.1	PA	6	7	71	68.09	71.85	70.90	0.24	4000	28	2	2/5
SCF/PP	17.6	PU[f]	6	7	64	66.98	70.64	63.57	0.2	4000	28	1	1
SCF/PP + MAPP	17.6	PU	6	7	83	66.98	70.64	82.66	0.32	4000	28	2	1
SGF[e]/PP	13	PA	4.5	10	42	55.39	69.09	42.97	0.1	2600	28	1	1/2
SGF/PP + MAPP	13	PA	4.5	10	70	55.39	69.09	96.96	0.3	2600	28	2	1
SGF/PP	13	PP[b]	4.5	14	54	56.99	41.49	53.87	0.14	2600	28	1	7/10
SGF/PP + MAPP	13	PP	4.5	14	66	56.99	41.49	65.88	0.21	2600	28	2	1/10

[a] Short Carbon Fibers.
[b] Polypropylene.
[c] Maleic anhydride-grafted polypropylene.
[d] Polyamide.
[e] Short Glass Fibers.
[f] Polyurethane.

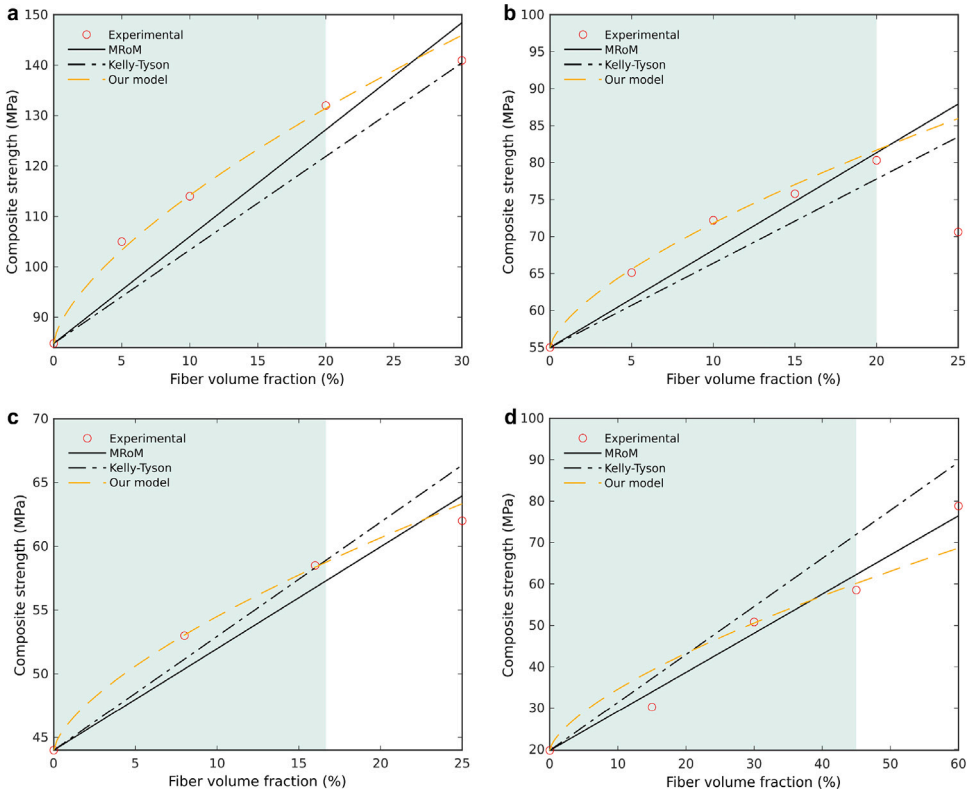

Fig. 8. Model predictions compared with experimental from the literature: (a) Zhao et al. (2018), (b) Nayak et al. (2023), (c) Fu et al. (2000), and (d) EL-Wazery et al. (2017).

4. Conclusion

As one of the most crucial properties of FRPCs, an accurate prediction of tensile strength is necessary to anticipate failures during service. For this purpose, classical models have been widely used owing to their relative accuracy and simplicity. While continuum-based models in the literature provide better physical interpretation, their reliance on numerous parameters and mathematical complexity restrict their widespread use. Therefore, we introduced a sensitive equation for predicting tensile strength in FRPCs with unidirectional fiber alignment.

This model quantitatively accounts for the impact of chemical bonding in enhancing interfacial adherence, eliminating the need to rely on the Interfacial Shear Strength (IFSS), which is often challenging and tedious to characterize. Extensive validation of the model across a diverse range of FRPC systems, using experimental data from the literature, has demonstrated its plausibility and accuracy. Our model captures the complex interplay among different constituents by introducing a new exponential variable that considers the effect of chemical bonding resulting from fiber surface treatments, sizing, and/or the addition of coupling agents in a layered fiber–matrix interphase.

Results showed that our model effectively captures the nonlinear behavior of FRPCs by controlling load-bearing capabilities as interphase strength varies throughout its thickness. Compared with existing experimental data, our model displayed more accurate predictions across a reasonable range of volume fractions than classical models. Furthermore, our parametric analysis supports the following constructive insights:

- Strong fibers do not necessarily introduce strong interphase at low Z values

- Thicker interphases do not necessarily improve the load transfer capabilities of composites. It is essential to optimize the interphase between the fiber and matrix to accurately represent the behavior of composites, agreeing with general perception. For this, our exponential variable can serve as an interphase quality measure.
- Our parameter K effectively accounts for the presence of chemical treatments as its variation in magnitude influences the final value of our new exponential variable.

From a practical point of view, our model presents an alternative solution for predicting the strength of composites, with the notable advantage that all its parameters can be easily obtained from technical sheets and/or the literature. Moreover, beyond offering valuable insights into the complex role of interphases in overall performance, this model serves as a practical tool for designing high-performance FRPCs with optimized tensile strength and durability.

CRediT authorship contribution statement

Jesus A. Rodriguez-Morales: Writing – original draft, Visualization, Validation, Methodology, Investigation, Formal analysis, Conceptualization. **Chentong Gao:** Writing – review & editing, Formal analysis, Conceptualization. **Huiyu Sun:** Writing – review & editing, Supervision, Conceptualization.

Declaration of Generative AI and AI-assisted technologies in the writing process

During the preparation of this work, the author(s) used ChatGPT in order to improve the grammar and readability of the text. After using this tool/service, the author(s) reviewed and edited the content as needed and take(s) full responsibility for the content of the publication.

Declaration of competing interest

We declare that we do not have any commercial or associative interest that represents a conflict of interest in connection with the work submitted.

Acknowledgments

This work is supported by the National Natural Science Foundation of China (Grant No. : 12372071), the Aeronautical Science Fund (Grant No. : 2022Z055052001), the Fund of Prospective Layout of Scientific Research for Nanjing University of Aeronautics and Astronautics, and the China Scholarship Council (CSC) (Scholarship Nos.: 2021GXZ008546, CSC202306830079).

Appendix A. Supplementary data

Supplementary material related to this article can be found online at https://doi.org/10.1016/j.euromechsol.2024.105533.

Data availability

All data that support the findings of this study are included within the article (and any supplementary files).

References

AhmadvashAghbash, S., Breite, C., Mehdikhani, M., Swolfs, Y., 2022. Longitudinal debonding in unidirectional fibre-reinforced composites: Numerical analysis of the effect of interfacial properties. Compos. Sci. Technol. 218, 109117.
Cox, H., 1952. The elasticity and strength of paper and other fibrous materials. Br. J. Appl. Phys. 3 (3), 72.
Dey, M., Deitzel, J., Gillespie, Jr., J., Schweiger, S., 2014. Influence of sizing formulations on glass/epoxy interphase properties. Composites A 63, 59–67.
Din, K., Hashemi, S., 1997. Influence of short-fibre reinforcement on the mechanical and fracture behaviour of polycarbonate/acylonitrile butadiene styrene polymer blend. J. Mater. Sci. 32, 375–387.
Dorigato, A., Dzenis, Y., Pegoretti, A., 2013. Filler aggregation as a reinforcement mechanism in polymer nanocomposites. Mech. Mater. 61, 79–90.
Downing, T., Kumar, R., Cross, W., Kjerengtroen, L., Kellar, J., 2000. Determining the interphase thickness and properties in polymer matrix composites using phase imaging atomic force microscopy and nanoindentation. J. Adhes. Sci. Technol. 14 (14), 1801–1812.
Duarte Garcia, M., Isaza Merino, C.A., Patiño Arcila, I.D., 2023. Analytical models for the effective tensile strength of nanocomposites: a comprehensive review. J. Braz. Soc. Mech. Sci. Eng. 45 (2), 105.
EL-Wazery, M.S., EL-Elamy, M.I., Zoalfakar, S.H., 2017. Mechanical properties of glass fiber reinforced polyester composites. Int. J. Appl. Sci. Eng. 14, 121–131.
Fard, M.Y., Raji, B., Pankretz, H., 2020. Time-scale through-thickness interphase in polymer matrix composites including hygrothermal treatment. Polym. Test. 83, 106365.
Franco-Marquès, E., Méndez, J., Pèlach, M., Vilaseca, F., Bayer, J., Mutjé, P., 2011. Influence of coupling agents in the preparation of polypropylene composites reinforced with recycled fibers. Chem. Eng. J. 166 (3), 1170–1178.
Fu, S.-Y., Lauke, B., 1996. Effects of fiber length and fiber orientation distributions on the tensile strength of short-fiber-reinforced polymers. Compos. Sci. Technol. 56 (10), 1179–1190.
Fu, S.-Y., Lauke, B., Mäder, E., Yue, C.-Y., Hu, X., 2000. Tensile properties of short-glass-fiber-and short-carbon-fiber-reinforced polypropylene composites. Composites A 31 (10), 1117–1125.
Gao, S.-L., Mäder, E., 2002. Characterisation of interphase nanoscale property variations in glass fibre reinforced polypropylene and epoxy resin composites. Compos. A 33 (4), 559–576.
Gao, S.-L., Mäder, E., Zhandarov, S.F., 2004. Carbon fibers and composites with epoxy resins: Topography, fractography and interphases. Carbon 42 (3), 515–529.
Goh, K., Aspden, R.M., Hukins, D.W.L., 2004. Finite element analysis of stress transfer in short-fibre composite materials. Compos. Sci. Technol. 64 (9), 1091–1100.
Gu, Y., Li, M., Wang, J., Zhang, Z., 2010. Characterization of the interphase in carbon fiber/polymer composites using a nanoscale dynamic mechanical imaging technique. Carbon 48 (11), 3229–3235.
Han, S.H., Oh, H.J., Kim, S.S., 2014. Evaluation of fiber surface treatment on the interfacial behavior of carbon fiber-reinforced polypropylene composites. Composites B 60, 98–105.
Hashimoto, M., Okabe, T., Sasayama, T., Matsutani, H., Nishikawa, M., 2012. Prediction of tensile strength of discontinuous carbon fiber/polypropylene composite with fiber orientation distribution. Composites A 43 (10), 1791–1799.
He, M., Xu, P., Zhang, Y., Liu, K., Yang, X., 2020. Phthalocyanine nanowires@GO/carbon fiber composites with enhanced interfacial properties and electromagnetic interference shielding performance. Chem. Eng. J. 388, 124255.
Huang, H.-B., Huang, Z.-M., 2020. Micromechanical prediction of elastic-plastic behavior of a short fiber or particle reinforced composite. Composites A 134, 105889.
Huang, Z.-M., Zhang, C.-C., Xue, Y.-D., 2019. Stiffness prediction of short fiber reinforced composites. Int. J. Mech. Sci. 161, 105068.
Jancar, J., 2008. Review of the role of the interphase in the control of composite performance on micro-and nano-length scales. J. Mater. Sci. 43, 6747–6757.
Kelly, A., Davies, G., 1965. The principles of the fibre reinforcement of metals. Metall. Rev. 10 (1), 1–77.
Kim, J.-K., Mai, Y.-W., 1998. Engineered Interfaces in Fiber Reinforced Composites. Elsevier.
Kim, J.-K., Sham, M.-L., Wu, J., 2001. Nanoscale characterisation of interphase in silane treated glass fibre composites. Compos. A 32 (5), 607–618.
Kundalwal, S., Kumar, S., 2016. Multiscale modeling of stress transfer in continuous microscale fiber reinforced composites with nano-engineered interphase. Mech. Mater. 102, 117–131.
Lee, C., Hwang, W., 1998. Modified rule of mixtures for prediction of tensile strength of unidirectional fiber-reinforced composites. J. Mater. Sci. Lett. 17 (1601), 1601–1603.
Li, Y., Li, W., Deng, Y., Shao, J., Ma, J., Tao, Y., Kou, H., Zhang, X., Zhang, X., Chen, L., et al., 2018. Temperature-dependent longitudinal tensile strength model for short-fiber-reinforced polymer composites considering fiber orientation and fiber length distribution. J. Mater. Sci. 53 (17), 12190–12202.
Li, Y., Li, W., Ma, J., Zheng, S., Zhao, Z., Yang, M., Dong, P., Chen, L., 2020. Temperature dependent longitudinal tensile strength model of unidirectional fiber reinforced polymer composites considering the effect of matrix plasticity. Extreme Mech. Lett. 40, 100963.

Li, Y., Li, W., Shao, J., Deng, Y., Kou, H., Ma, J., Zhang, X., Zhang, X., Chen, L., Qu, Z., 2019. Modeling the effects of interfacial properties on the temperature dependent tensile strength of fiber reinforced polymer composites. Compos. Sci. Technol. 172, 74–80.

Li, M., Wen, X., Liu, J., Tang, T., 2014. Synergetic effect of epoxy resin and maleic anhydride grafted polypropylene on improving mechanical properties of polypropylene/short carbon fiber composites. Composites A 67, 212–220.

Liu, L., Jia, C., He, J., Zhao, F., Fan, D., Xing, L., Wang, M., Wang, F., Jiang, Z., Huang, Y., 2015. Interfacial characterization, control and modification of carbon fiber reinforced polymer composites. Compos. Sci. Technol. 121, 56–72.

Ma, L., Meng, L., Wu, G., Wang, Y., Zhao, M., Zhang, C., Huang, Y., 2015. Effects of bonding types of carbon fibers with branched polyethyleneimine on the interfacial microstructure and mechanical properties of carbon fiber/epoxy resin composites. Compos. Sci. Technol. 117, 289–297.

Mäder, E., Pisanova, E., 2000. Characterization and design of interphases in glass fiber reinforced polyproplyene. Polym. Compos. 21 (3), 361–368.

Mao, R.-S., Huang, Z.-M., Wang, Z.-W., 2021. Predicting strength of a unidirectional composite containing interface crack. Compos. Sci. Technol. 207, 108665.

Mohandesi, J.A., Sangghaleh, A., Nazari, A., Pourjavad, N., 2011. Analytical modeling of strength in randomly oriented PP and PPTA short fiber reinforced gypsum composites. Comput. Mater. Sci. 50 (5), 1619–1624.

Montes-Morán, M., Van Hattum, F., Nunes, J., Martínez-Alonso, A., Tascón, J., Bernardo, C., 2005. A study of the effect of plasma treatment on the interfacial properties of carbon fibre–thermoplastic composites. Carbon 43 (8), 1795–1799.

Montes-Morán, M.A., Young, R.J., 2002. Raman spectroscopy study of high-modulus carbon fibres: effect of plasma-treatment on the interfacial properties of single-fibre–epoxy composites: Part II: Characterisation of the fibre–matrix interface. Carbon 40 (6), 857–875.

Nayak, S., Samal, P., Malla, C., Pradhan, M.K., Khuntia, S.K., Mohapatra, J., Jena, P.K., Patra, S.K., Nayak, B.B., Swain, S., 2023. Enhancement of mechanical, thermal and morphological properties of eleusine indica grass fiber reinforced epoxy composites. J. Nat. Fibers 20 (1).

Pan, Y., Weng, G., Meguid, S., Bao, W., Zhu, Z., Hamouda, A., 2013. Interface effects on the viscoelastic characteristics of carbon nanotube polymer matrix composites. Mech. Mater. 58, 1–11.

Papanicolaou, G., Anifantis, N., Keppas, L., Kosmidou, T.V., 2007. Stress analysis of short fiber-reinforced polymers incorporating a hybrid interphase region. Compos. Interfaces 14 (2), 131–152.

Rangaraj, S., Bhaduri, S., 1994. A modified rule-of-mixtures for prediction of tensile strengths of unidirectional fibre-reinforced composite materials. J. Mater. Sci. 29, 2795–2800.

Rivas-Menchi, A., Herrera-Franco, P.J., Valadez-González, A., Arcos-Alomía, A., 2024. Enhancing interfacial shear strength with tailored carbon nanotube orientations: A micromechanical hierarchical model of single fiber fragmentation tests. Mater. Today Commun. 38, 108104.

Ryu, H.J., Cha, S.I., Hong, S.H., 2003. Generalized shear-lag model for load transfer in SiC/Al metal-matrix composites. J. Mater. Res. 18 (12), 2851–2858.

Sharma, M., Gao, S., Mäder, E., Sharma, H., Wei, L.Y., Bijwe, J., 2014. Carbon fiber surfaces and composite interphases. Compos. Sci. Technol. 102, 35–50.

Shokrieh, M., Moshrefzadeh-Sani, H., 2017. A novel laminate analogy to calculate the strength of two-dimensional randomly oriented short-fiber composites. Compos. Sci. Technol. 147, 22–29.

Sørensen, B.F., Lilholt, H., 2016. Fiber pull-out test and single fiber fragmentation test-analysis and modelling. In: IOP Conference Series: Materials Science and Engineering. Vol. 139, IOP Publishing, 012009.

Sun, Z., Guo, F.-L., Wu, X.-P., Li, Y.-Q., Zeng, W., Chen, Q., Huang, T., Huang, P., Fu, Y.-Q., Ma, X.-Y., et al., 2022. Experimental and simulation investigations of the effect of hybrid GO-thermoplastic polyimide sizing on the temperature-dependent tensile behavior of short carbon fiber/polyetherimide composites. Compos. Sci. Technol. 218, 109166.

Sun, Z., Li, Y.-Q., Huang, P., Cao, H.-J., Zeng, W., Li, J., Li, F., Sun, B.-G., Shi, H.-Q., Zhou, Z.-l., et al., 2021. Temperature-dependent mechanical properties of polyetherimide composites reinforced by graphene oxide-coated short carbon fibers. Compos. Struct. 270, 114075.

Unterweger, C., Brüggemann, O., Fürst, C., 2014. Effects of different fibers on the properties of short-fiber-reinforced polypropylene composites. Compos. Sci. Technol. 103, 49–55.

Unterweger, C., Duchoslav, J., Stifter, D., Fürst, C., 2015. Characterization of carbon fiber surfaces and their impact on the mechanical properties of short carbon fiber reinforced polypropylene composites. Compos. Sci. Technol. 108, 41–47.

Wong, K.H., Mohammed, D.S., Pickering, S.J., Brooks, R., 2012. Effect of coupling agents on reinforcing potential of recycled carbon fibre for polypropylene composite - ScienceDirect. Compos. Sci. Technol. 72 (7), 835–844.

Wu, Y., Wang, Z., Xu, L., Wang, H., Peng, S., Zheng, L., Yang, Z., Wu, L., Miao, J.-T., 2021. Preparation of silver-plated carbon nanotubes/carbon fiber hybrid fibers by combining freeze-drying deposition with a sizing process to enhance the mechanical properties of carbon fiber composites. Composites A 146, 106421.

Yamamoto, G., Koizumi, K., Nakamura, T., Hirano, N., Okabe, T., 2021. Tensile-strength-controlling factors in unidirectional carbon fiber reinforced plastic composites. Composites A 140, 106140.

Yamamoto, G., Onodera, M., Koizumi, K., Watanabe, J., Okuda, H., Tanaka, F., Okabe, T., 2019. Considering the stress concentration of fiber surfaces in the prediction of the tensile strength of unidirectional carbon fiber-reinforced plastic composites. Composites A 121, 499–509.

Yamamoto, G., Oshima, K., Ramadhan, R.A., Lim, T., Megra, Y.T., Suk, J.W., Watanabe, J., Okuda, H., Tanaka, F., 2024. Tensile strength prediction of unidirectional polyacrylonitrile (PAN)-based carbon fiber reinforced plastic composites considering stress distribution around fiber break points. Composites A 183, 108234.

Yan, X., Yang, Y., Hamada, H., 2018. Tensile properties of glass fiber reinforced polypropylene composite and its carbon fiber hybrid composite fabricated by direct fiber feeding injection molding process. Polym. Compos. 39 (10), 3564–3574.

Yang, M., Li, W., Li, Y., Zhang, X., Zhao, Z., He, Y., Dong, P., Zheng, S., Xu, W., 2021. Theoretical characterization of the temperature-dependent ultimate tensile strength of short-fiber-reinforced polymer composites. Polym. Compos. 42 (8), 3933–3942.

Yang, Y., Pang, J., Dai, H.-L., Xu, X.-M., Li, X.-Q., Mei, C., 2019. Prediction of the tensile strength of polymer composites filled with aligned short fibers. J. Reinf. Plast. Compos. 38 (14), 658–668.

Yazdani, H., Morshedian, J., Khonakdar, H., 2006. Effects of silane coupling agent and maleic anhydride-grafted polypropylene on the morphology and viscoelastic properties of polypropylene–mica composites. Polym. Compos. 27 (5), 491–496.

Zare, Y., 2014. Determination of polymer–nanoparticles interfacial adhesion and its role in shape memory behavior of shape memory polymer nanocomposites. Int. J. Adhes. Adhes. 54, 67–71.

Zare, Y., 2016. Modeling approach for tensile strength of interphase layers in polymer nanocomposites. J. Colloid Interface Sci. 471, 89–93.

Zhang, X., Li, W., Shao, L.-H., Li, Y., Wang, J., 2024. Micromechanics-based modeling of temperature-dependent effective moduli of fiber reinforced polymer composites with interfacial debonding. Composites A 108049.

Zhao, Z.-K., Du, S.-S., Li, F., Xiao, H.-M., Li, Y.-Q., Zhang, W.-G., Hu, N., Fu, S.-Y., 2018. Mechanical and tribological properties of short glass fiber and short carbon fiber reinforced polyethersulfone composites: A comparative study. Compos. Commun. 8, 1–6.

Zheng, H., Zhang, W., Li, B., Zhu, J., Wang, C., Song, G., Wu, G., Yang, X., Huang, Y., Ma, L., 2022. Recent advances of interphases in carbon fiber-reinforced polymer composites: A review. Composites B 233, 109639.